technologies

MDPI

Article

Non-Contact Platform for the Assessment of Physical Function in Older Adults: A Pilot Study

Ana Sobrino-Santos [1,2], Pedro Anuarbe [1,2], Carlos Fernandez-Viadero [2,3], Roberto García-García [4], José Miguel López-Higuera [1,2,5], Luis Rodríguez-Cobo [1,2,5,*,†] and Adolfo Cobo [1,2,5,†]

1 Photonics Engineering Group, Universidad de Cantabria, 39005 Santander, Spain
2 Instituto de Investigación Sanitaria Valdecilla (IDIVAL), 39011 Santander, Spain
3 Psychiatry Service, Marqués de Valdecilla University Hospital, 39011 Santander, Spain
4 Ambar Telecomunicaciones S.L., 39011 Santander, Spain
5 CIBER de Bioingeniería, Biomateriales y Nanomedicina, Instituto de Salud Carlos III, 28029 Madrid, Spain
* Correspondence: luis.rodriguez@unican.es
† These authors contributed equally to this work and share senior authorship.

Abstract: In the context of global population aging, identifying reliable, objective tools to assess physical function and postural stability in older adults is increasingly important to mitigate fall risk. This study presents a non-contact platform that uses a Microsoft Azure Kinect depth camera to evaluate functional performance related to lower-limb muscular capacity and static balance through self-selected depth squats and four progressively challenging stances (feet apart, feet together, semitandem, and tandem). By applying markerless motion capture algorithms, the system provides key biomechanical parameters such as center of mass displacement, knee angles, and sway trajectories. A comparison of older and younger individuals showed that the older group tended to perform shallower squats and exhibit greater mediolateral and anteroposterior sway, aligning with age-related declines in strength and postural control. Longitudinal tracking also illustrated how performance varied following a fall, indicating potential for ongoing risk assessment. Notably, in 30 s balance trials, the first 10 s often captured meaningful differences in stability, suggesting that short-duration stance tests can reliably detect early signs of imbalance. These findings highlight the feasibility of low-cost, user-friendly depth-camera technologies to complement traditional clinical measures and guide targeted fall-prevention strategies in older populations.

Keywords: functional assessment; depth cameras; squat; balance; falls; biomechanics

Academic Editors: Daniele Giansanti and Luc de Witte

Received: 9 April 2025
Revised: 27 May 2025
Accepted: 30 May 2025
Published: 2 June 2025

Citation: Sobrino-Santos, A.; Anuarbe, P.; Fernandez-Viadero, C.; García-García, R.; López-Higuera, J.M.; Rodríguez-Cobo, L.; Cobo, A. Non-Contact Platform for the Assessment of Physical Function in Older Adults: A Pilot Study. *Technologies* **2025**, *13*, 225. https://doi.org/10.3390/technologies13060225

1. Introduction

Worldwide populations are aging at unprecedented rates. By 2030, it is estimated that one in six people globally will be 60 years or older, and the global count of individuals over 60 is expected to rise from 1.0 billion in 2020 to 1.4 billion [1]. By 2050, that number is projected to double to 2.1 billion [1]. Additionally, the population aged 80 and above will triple from 2020 to 2050, reaching 426 million [1]. This demographic shift creates a multitude of challenges in public health, particularly with increased risks of falls, frailty, and dependency.

Falls among older adults represent a major public health issue, with approximately 23.4% of those aged 65 and older experiencing at least one fall each year [2]. These incidents can lead to serious consequences, making falls a leading cause of injuries, hospitalizations, and even mortality in the elderly [3]. Beyond the immediate injuries, falls can precipitate long-term declines in function and independence, leading to sedentary behavior and a reduced quality of life for seniors [4]. Consequently, fall prevention is essential for enhancing healthy life expectancy and reducing healthcare system strain [5].

In this context, physical function assessments and biomechanical movement analysis are valuable tools for evaluating an older person's mobility and fall risk. Objective performance measures of gait and balance have well-documented clinical relevance—for example, slow walking speed or difficulty in chair-rise tests are associated with higher rates of future falls, disability, hospitalization, and even mortality [6]. Muscle weakness and impaired balance are well-established risk factors for falls [5]. Traditionally, functional assessments (such as static balance tests, gait analysis, or sit-to-stand tests) rely on time-based measurements or qualitative observation by professionals, which may limit the accuracy and objectivity of the evaluation.

Many widely used functional tests provide only coarse summary outcomes, such as the time to complete a Timed Up-and-Go (TUG) test [7], the number of repetitions in a chair stand test [8] or the composite score of the Short Physical Performance Battery (SPPB) [9], potentially overlooking subtle deficits in movement quality or motor control. Researchers have noted that objective sensor-based measures can be more sensitive than coarse clinical tests for detecting balance and gait impairments. For instance, an instrumented Timed Up-and-Go (iTUG) that uses wearable sensors can capture additional parameters beyond completion time, thereby identifying nuanced performance variables and improving fall-risk prediction. This evidence underscores the need for more objective, data-rich methods in geriatric care [10].

Markerless motion capture techniques offer a promising solution for objective, non-invasive, and high-resolution assessments in clinical and home settings. Various systems—including force platforms, wearable inertial sensors, and optical depth cameras—enable detailed quantification of biomechanical parameters, facilitating improved monitoring of functional status. Non-contact markerless systems use external cameras to track body kinematics without any sensors attached to the person. These vision-based devices capture three-dimensional movements of the body without requiring physical markers on the subject. Depth-sensing cameras in particular can directly measure distances to the body and construct a skeletal model in real time, providing rich motion data while being unobtrusive for the user.

Among depth cameras, the Microsoft Azure Kinect stands out as an evolution of the Kinect line, offering higher accuracy in 3D reconstruction, an improved working range, and an updated Software Development Kit (SDK). Several studies [11,12] have reported its effectiveness in quantifying gait, posture, and balance parameters, with relatively simple implementation and lower cost compared to traditional laboratory-based systems. This capability opens up opportunities to deploy objective mobility assessments in environments such as community clinics, nursing homes, or even patients' homes, which is particularly beneficial for monitoring at-risk older populations. Nevertheless, despite these technological advances, relatively few studies to date have focused on deploying markerless motion capture for comprehensive geriatric assessment. Recent reviews highlight that further research is still needed to establish the clinical usefulness of such markerless systems for quantifying functional performance in real-world older adult populations [13].

The present work proposes a non-contact functional evaluation platform based on a low-cost depth sensor (Azure Kinect), aimed at older adults. The system is designed to capture key biomechanical metrics during two simple physical function tests: self-selected depth squat exercise and static balance tests in four different stances. These test activities target indicators of lower-limb muscular capacity (e.g., squat depth) and balance—the domains most pertinent to mobility and fall risk in seniors—and the use of a markerfree sensor allows them to be evaluated objectively without the need for wearables or extensive setup.

The objectives are (1) to demonstrate the technical feasibility of using a non-contact depth sensor (Azure Kinect (Microsoft Corp., Redmond, WA, USA)) to measure relevant variables of physical function (balance and lower limb strength) in older adults, (2) to systematically compare these measurements with data from young healthy subjects, and (3) to explore the potential of this platform for early detection of physical decline. Through this approach, we aim to show that a markerless depth camera system can effectively provide accurate and actionable assessments of balance and lower-extremity function in older individuals.

2. Materials and Methods

2.1. System Design and Architecture

The proposed platform consists of a non-invasive evaluation system that integrates motion capture hardware and data processing software. The system is composed of the following: (i) an Azure Kinect depth sensor responsible for capturing the participant's movement in three dimensions and (ii) a software module for real-time visualization, data processing and biomechanical metric calculation. In Figure 1, a schematic of the overall architecture and data flow is shown.

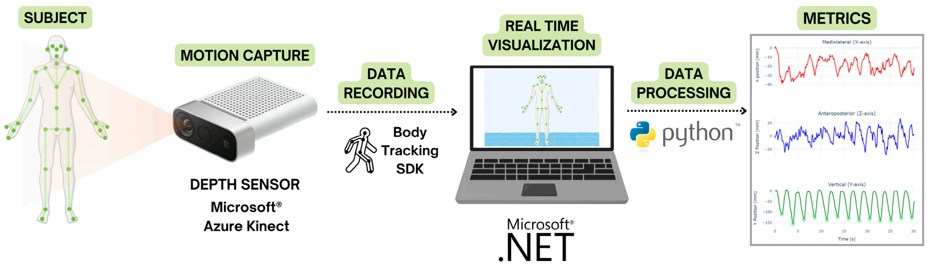

Figure 1. Overall architecture and data flow.

2.1.1. Azure Kinect

The Azure Kinect (Microsoft®) [14] is the system's central component. This next-generation device includes a 12-megapixel RGB camera, a 1-megapixel Time-of-Flight (ToF) depth sensor, an integrated inertial measurement unit (IMU), and an array of 7 microphones (Figure 2). The depth sensor emits an infrared pattern and measures the time-of-flight of the light to calculate distances, thus producing a depth map of the scene in real time. Unlike the previous Kinect v2 (Xbox One), Azure Kinect offers higher resolution and a wider field of view, improving spatial and temporal accuracy in human skeleton tracking. These characteristics make it suitable for capturing the key body movements relevant to functional evaluations.

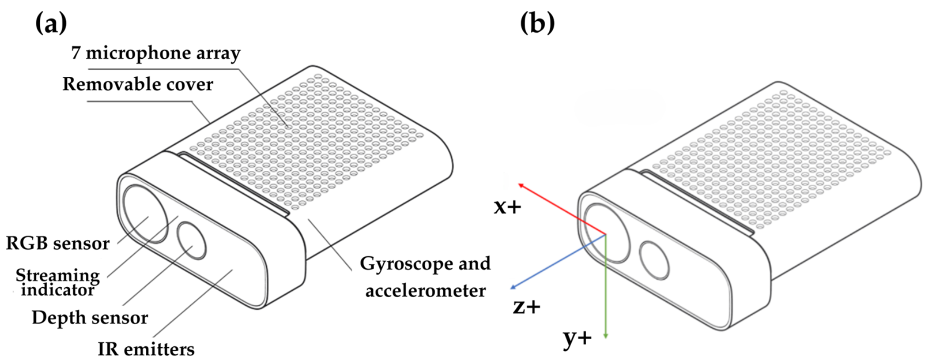

Figure 2. Azure Kinect (**a**) components and (**b**) 3D-coordinate system [14].

To obtain the subject's posture, the platform uses Microsoft's body tracking SDK, which estimates the positions of a series of skeletal joints in each captured frame. Specifically, Azure Kinect returns 3D coordinates for 32 body joints—including the head, trunk, upper and lower extremities—at a frequency of up to 30 frames per second. This sampling rate (30 Hz) is sufficient for analyzing human movements in the selected tests since the main components of movement during balance and gait occur at low frequencies (generally below ~2–3 Hz) [15]. Biomechanical studies have shown, for instance, that rapid oscillations of postural sway rarely exceed 2 Hz, so the sensor's 30 Hz sampling covers the necessary dynamic range. In our study, however, we opted to record at 15 frames per second to reduce graphics-processing-unit (GPU) computational requirements; given that postural oscillations seldom exceed 2 Hz, this reduced rate is adequate to capture the necessary dynamics without demanding excessive processing power.

In its default configuration, the sensor's coordinate system is defined with the X axis running horizontally (with positive values toward the right of the camera), the Y axis oriented vertically (with positive values directed downward), and the Z axis representing depth (with positive values increasing away from the sensor), as shown in Figure 2. For the purposes of our biomechanical analyses, the raw Y values are later inverted so that upward movements are represented by positive values, thus facilitating the interpretation of vertical displacements during exercise.

The Azure Kinect was selected for this study due to its cost-effectiveness, ease of deployment, and enhanced tracking accuracy compared to earlier Kinect models.

2.1.2. Software Implementation

The software module of the platform was developed using a combination of languages: C# (v7.3) and Python (v3.12.4).

C# was used to interface with the Azure Kinect SDKs and perform, using the .NET framework, real-time data acquisition and preview of the tracked skeleton, allowing the clinician to verify that the subject is correctly positioned before data collection begins. Using the official Azure Kinect and Body Tracking SDKs, a simple desktop application was created in C# that initializes the camera, detects the subject, and begins recording the skeleton sequence when the evaluator indicates. This module not only allows the selection of the test type (squat or balance) to label the corresponding data but also continuously records the joint positions along with timestamps while the subject performs the exercise. Upon completion, the raw data are exported to CSV files, including joint identifiers, coordinates (position and orientation), timestamp, and a test label.

Python was used for data processing and metric calculation, thanks to its scientific ecosystem for efficient data manipulation (libraries like Numpy (v2.0), Pandas (v2.2.2) and SciPy (v1.14.1)) and visualization tools (libraries like Matplotlib (v3.9.1) and Plotly (v.5.24.1)). The software architecture follows a workflow in which the raw Kinect data (joint coordinates per frame) are stored and later processed by Python scripts that compute the biomechanical metrics.

In summary, the platform's design enables a rapid and objective evaluation: the older adult positions himself in front of the sensor and performs the designated exercises without needing markers or wearable devices; the system records the movement and, within seconds, calculates quantitative physical performance metrics. This ease of use and speed are essential for application in busy clinical settings.

2.2. Selected Exercises for Evaluation

Based on the experience provided by clinical personnel, two complementary functional tests were selected: (a) a dynamic lower-limb functional exercise (self-selected depth squats) and (b) static balance tests in progressively challenging stances (see Figures 3 and 4). The combination of these tests seeks to evaluate fundamental aspects of function in older adults: leg strength and postural stability.

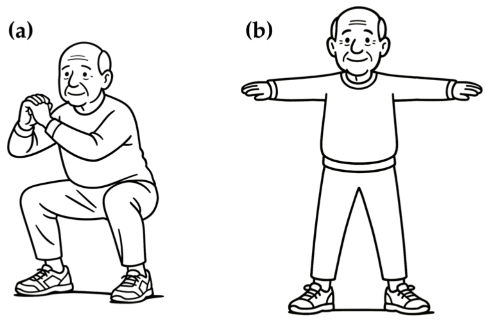

Figure 3. Illustration of the selected exercises: (**a**) self-selected depth squats and (**b**) static balance.

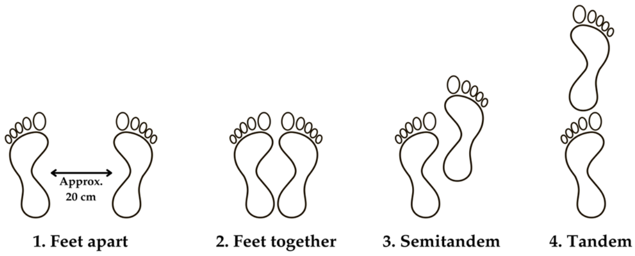

Figure 4. Overview of static balance stances.

2.2.1. Self-Selected Depth Squats

The first exercise consists of performing continuous self-selected depth squats for a duration of 30 s, according to the participant's capacity and comfort, without specifying a fixed depth; that is, each older adult descends as far as they feel safe and stable.

Squats are widely recognized as a fundamental movement for assessing lower-limb functional capacity related to strength rather than measuring muscle force directly. They involve coordinated activation of the quadriceps, hamstrings, and gluteal muscles, making them an effective proxy for evaluating the overall strength and mobility of the lower extremities.

In our study, we employ a self-selected depth squat, which allows evaluation of the effective range of motion and strength without forcing the participant into a posture that might be uncomfortable or risky for their joints. Unlike standardized squat protocols that may use a fixed target (e.g., sitting down on a chair), the self-selected approach respects individual variability in joint range and strength. This is particularly important for older adults, who often exhibit reduced flexibility and joint discomfort when forced to achieve a predetermined depth. By allowing a free-depth squat, our system captures the authentic functional performance of each participant, thereby providing a more accurate reflection of their lower-limb strength and mobility. Moreover, variations in squat depth can reveal asymmetries or compensatory strategies that might not be evident with a constrained movement.

2.2.2. Static Balance

The second part of the evaluation corresponds to static balance tests with progressively challenging stances. Four standing postures were selected—each with increasing difficulty—similar to those used in clinical balance assessments [9]. The selected stances, in order of increasing challenge, were as follows: (1) Feet apart (standing with feet shoulder-width apart, approximately 20 cm), (2) Feet together (both feet placed side-by-side),

(3) Semitandem (one foot slightly ahead, with the heel of the front foot approximately halfway along the rear foot), and (4) Tandem (right foot directly in front of the left, heel-to-toe). These postures challenge the balance system progressively by reducing the base of support (see Figure 4).

The four selected stances allow multilevel evaluation of balance. The feet apart stance is very stable and almost all independent older adults can maintain it easily; it serves as a baseline reference for sway. When feet are together, the base is reduced, and slight increases in Center of Mass (CoM) oscillations are typically observed. The semitandem stance demands greater lateral balance and serves as an intermediate step; many older adults can hold it, though with more effort. Finally, the tandem stance is considerably challenging; failing to maintain 10 s in tandem is common in those with compromised balance. These stances are directly derived from validated clinical tests: for instance, the SPPB [9] measures the ability to maintain 10 s in these positions. However, our platform not only assesses whether a subject can maintain the posture for 10 s but also quantifies their movement during the task. Subtle differences in control can be captured; for example, two individuals might both maintain 10 s in tandem, but one does so almost motionless while the other sways noticeably; clinically they would receive the same score, but biomechanically their balance differs. The platform quantifies these differences using the metrics described in Section 2.3.

2.3. Metrics

2.3.1. Center of Mass (CoM)

The calculation of the overall CoM is central to the analysis of human movement and postural stability. In this study, we adopt an anthropometric model based on De Leva's modifications [16] to the classical segmental inertia parameters originally proposed by Zatsiorsky and Seluyanov [17]. According to this approach, the human body is divided into distinct segments—specifically, the trunk, thighs, shanks, and feet—with each segment assigned a specific percentage of the total body mass and a predetermined point of application representing its individual CoM (see Figure 5 and Table 1).

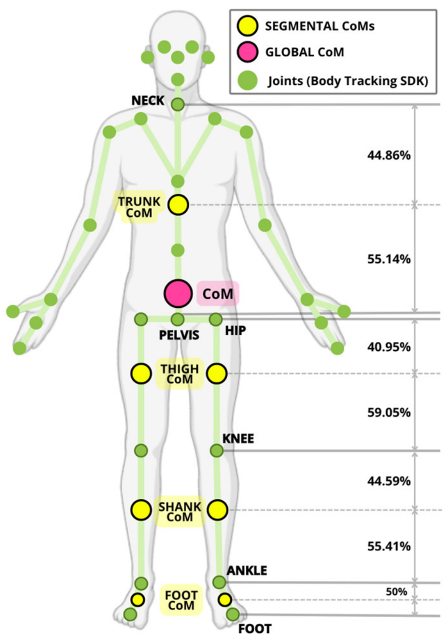

Figure 5. Segmental and Global CoMs based on De Leva's [16].

Table 1. Parameters for each unique segment.

Segment	Defining Joints	α (% of Length)	Relative Mass (kg) [1]
Trunk	PELVIS–NECK	55.14%	52.3
Thigh	HIP–KNEE	40.95%	17.0
Shank	KNEE–ANKLE	44.59%	5.2
Foot	ANKLE–FOOT	50%	1.65

[1] Renormalized masses to sum 100%.

For each segment i, the segmental CoM (CoM_i) is estimated by linear interpolation between the proximal and distal joint positions. For example, for the thigh, the CoM is calculated along the line joining the hip and knee, using a proportion α, that represents the percentage of the segment's length at which the CoM is located. Mathematically, if $\vec{r}_{proximal}$ and $\vec{r}_{distal}$ are the position vectors of the proximal and distal joints, respectively, then the CoM for that segment is given by:

$$CoM_i = \vec{r}_{proximal} + \alpha \times \left(\vec{r}_{distal} - \vec{r}_{proximal}\right) \quad (1)$$

The overall body CoM is subsequently determined as the weighted average of all segmental centers of mass:

$$CoM_{total} = \frac{\sum_i (m_i \times CoM_i)}{\sum_i m_i} \quad (2)$$

where m_i denotes the mass fraction of segment i. In this study, we have deliberately excluded the head and arms from the CoM calculation to focus on the dynamics of the lower limbs and trunk. This decision is supported by previous research [18] showing that upper-body segments (arms and head) contribute additional variability in the mediolateral (ML) direction of CoM motion, which may obscure subtle differences in lower-limb performance during tasks such as squatting and static balance. The accurate estimation of the CoM is fundamental as it underpins subsequent analyses, including the detection of squat events and the assessment of postural sway.

2.3.2. Joint Angles: Knee and Spine Alignment

Another set of metrics focuses on the key joint angles involved in the exercises: knee angle and a measure of spinal alignment. These parameters provide information on the subject's posture and technique during the movement, which is relevant for evaluating movement quality and potential compensations.

Knee angle is defined as the angle between the thigh and the shank. Using the coordinates of the hip, knee and ankle, the knee angle θ_{knee} is computed using the cosine law, via the dot product of the vectors representing the thigh ($\vec{v}_{thigh}$, hip to knee) and the shank ($\vec{v}_{shank}$, knee to ankle). That is:

$$\theta_{knee} = arcos\left(\frac{\vec{v}_{thigh} \cdot \vec{v}_{shank}}{\left\|\vec{v}_{thigh}\right\| \left\|\vec{v}_{shank}\right\|}\right) \quad (3)$$

This angle is approximately 180° when the leg is fully extended (standing upright) and decreases as the knee flexes (e.g., around 90° in a mid-depth squat). For each frame, the knee angle achieved in each leg is extracted and the minimum knee angle corresponds to the point of maximum flexion. This value serves as an indicator of squat depth complementary to the CoM descent: a lower minimum knee angle indicates greater flexion. For instance, if a subject only performs a shallow squat, their minimum knee angle might be around 140°, whereas a deeper squat might reach 100° or less.

Maintaining a straight back during squat is important to reduce injury risk and ensure that the load is borne by the legs. To quantify spinal posture, an index of back alignment was defined. The joints used are the pelvis, lumbar spine (spine_navel joint), thoracic spine (spine_chest joint), and neck. We then construct three sequential vectors:

- Vector 1 ($\vec{v}_1$): From the pelvis to the lumbar spine.
- Vector 2 ($\vec{v}_2$): From the lumbar spine to the thoracic spine.
- Vector 3 ($\vec{v}_3$): From the thoracic spine to the neck.

The angles between adjacent vectors are computed using the cosine law:

$$\theta_1 = arcos\left(\frac{\vec{v}_1 \cdot \vec{v}_2}{\left\|\vec{v}_1\right\|\left\|\vec{v}_2\right\|}\right)\theta_2 = arcos\left(\frac{\vec{v}_2 \cdot \vec{v}_3}{\left\|\vec{v}_2\right\|\left\|\vec{v}_3\right\|}\right) \tag{4}$$

If the spine were perfectly straight, these segments would be aligned and the angles would be close to 0°. To obtain a single index, the two angles are averaged and expressed as a deviation from perfect alignment, defined as:

$$Spine\ Alignment\ Index = 180^{\circ} - \frac{(\theta_1 + \theta_2)}{2} \tag{5}$$

Essentially, this value indicates how far the spine deviates from a straight line. A value near 0 would imply a very curved back (high $\theta_1 + \theta_2$), whereas higher values (e.g., 170°) indicate a straighter back. In our results, this index is reported in degrees; for example, an index of 175° suggests good alignment (almost straight spine, only 5° deviation on average per section), whereas 160° would indicate a notable forward bend during the squat. This calculation, while simplified (not distinguishing between lumbar or thoracic curvature), provides a quantitative measure of the subject's back posture during the exercise.

Together, the measures of knee angle and spinal alignment allow an assessment of the technique employed during the squat. This is important because, for example, a subject could achieve good depth (low CoM, knees around 100°) but at the expense of a heavily rounded back (low spine index), which is not ideal. Our metrics can detect such compensations. Similarly, if a subject has limited ankle or hip mobility, it may manifest as an abnormal posture that is reflected in these angles.

2.3.3. Symmetry Index

Movement symmetry is another important consideration, especially in bilateral exercises such as squats. Many older adults may exhibit differences in strength or mobility between their legs (for example, due to unilateral arthritis or past injuries), which could cause one leg to bear more load or have less flexion than the other during a squat. To quantify possible asymmetries, a Symmetry Index based on the knee angles was calculated.

The Symmetry Index (SI) is defined as the percentage difference between both legs relative to the mean value, using the common formula in biomechanics [19]:

$$\text{Symmetry Index} = \frac{\left|\theta_{\text{left}} - \theta_{\text{right}}\right|}{\frac{\theta_{\text{left}} + \theta_{\text{right}}}{2}} \times 100\% \tag{6}$$

where θ refers to the minimum knee angle reached during the squat for each side. This metric, widely used to quantify asymmetries in gait and movement, yields 0% if both sides are identical and increases as the difference grows. For example, if a subject flexes the left knee to 100° and the right to 110° at maximum depth, the SI would be $\frac{|100-110|}{(100+110)/2} \times 100 \approx 9.52\%$, indicating that one knee flexed about 9.5% less than the other.

2.3.4. Squat Detection and Squat Index

The system also performs automatic recognition of squat repetitions and extraction of the depth achieved in each. An algorithm was implemented to analyze the time series of the CoM to identify the movement cycles corresponding to each squat.

The vertical CoM signal (Y) (inverted for facilitating the interpretation) was chosen for detection because it exhibits a clear pattern: it decreases when lowering during a squat and increases when rising. In the CoM-Y signal, each complete squat appears as a valley (descent followed by ascent). SciPy's `find_peaks()` [20] function was used on the inverted signal ($-$CoM-Y). After an empirical tuning phase during the first two pilot sessions, the parameters were fixed for all subsequent recordings at prominence ≥ 20 mm, minimum inter-peak distance = 5 frames ($\approx$0.33 s at 15 Hz), and a height threshold of -20 mm. These settings avoided counting minor sub-movements or brief pauses as separate repetitions and reliably isolated the instant of greatest descent for each squat.

The initial standing position is a critical reference for calculating squat depth. In our methodology, this position was determined by averaging the first three maximum peaks of the CoM-Y signal, based on the rationale that at the end of each squat the user returns to their initial standing posture, at least during the first squats. Averaging these maximum peaks, rather than simply taking the very first CoM-Y data points, mitigates the potential error that might occur if the recording starts while the subject is already performing the first squat. This approach ensures a more robust estimation of the baseline standing position. Once the initial standing position is established, the algorithm identifies the instants (t_i) corresponding to the deepest points during each squat. The squat depth is then calculated as the difference between the CoM-Y value at the initial standing position and the CoM-Y minimum at t_i.

Figure 6 illustrates an example of squat detection in the CoM-Y signal. The figure shows how the valleys correspond to individual squats, and it demonstrates the process of identifying both the initial standing position and the lowest points during each squat repetition.

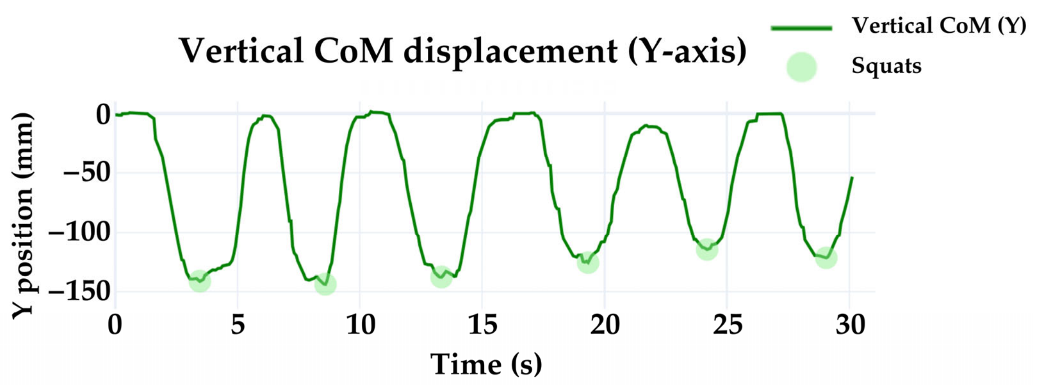

Figure 6. Example of squat detection in CoM Y-axis signal (participant ID6 (84 years, wheelchair)).

To capture both the quantity and quality of the squatting performance, we introduce a Squat Index. This index is calculated as the product of the number of correctly detected squats and the mean squat depth. By combining these two aspects—repetition count and effective range of motion—the Squat Index provides a more comprehensive measure of squatting performance. We formulate this idea as:

$$\text{Squat Index} = N_{squats} \times \overline{d} \tag{7}$$

where N_{squats} is the number of correctly detected squats and $\bar{d}$ is their mean vertical depth in millimeters. Expressing the Squat Index in the original depth unit (mm) keeps it directly interpretable: one deep squat (e.g., 200 mm) has the same Squat Index as two half-depth squats (2×100 mm).

2.3.5. Balance Analysis

For the static balance tests, the derived metrics focused on quantifying the subject's postural sway during each stance. From the CoM trajectory (described in Section 2.3.1), several indicators were extracted:

- Maximum mediolateral (ML) and anteroposterior (AP) displacement: The maximum distance that the CoM deviated laterally (ML) and front-to-back (AP) from the center during the test. This provides an idea of the range of oscillation. For example, an ML max value of 20 mm means the greatest lateral deviation was 2 cm. Higher values suggest greater episodes of imbalance.
- Mean absolute deviation: The average absolute distance of the CoM from the center in both ML and AP directions. This reflects the sustained level of instability. For instance, if someone oscillates constantly by ± 10 mm, the mean absolute deviation will be around 10 mm; if they hardly move from the center, it will be closer to 0.
- Elliptical confidence area (stabilographic area): The area of an ellipse that encompasses approximately 95% of the CoM trajectory was calculated. It was assumed that the distribution of CoM points is elliptical around the center. The standard deviations of the ML (σ_x) and AP (σ_z) positions were estimated. Then, applying a confidence factor (approximately 2.5), an ellipse with semi-axes $a = 2.5\sigma_x$ and $b = 2.5\sigma_z$ was constructed. The area of this ellipse is given by πab. This area (expressed in mm^2) serves as a measure to compare stability objectively: a smaller area implies the CoM remained within a small range, while a larger area indicates more dispersed oscillations. Each stance produces a different area. It is expected that more challenging stances will have larger areas (see Figure 7).

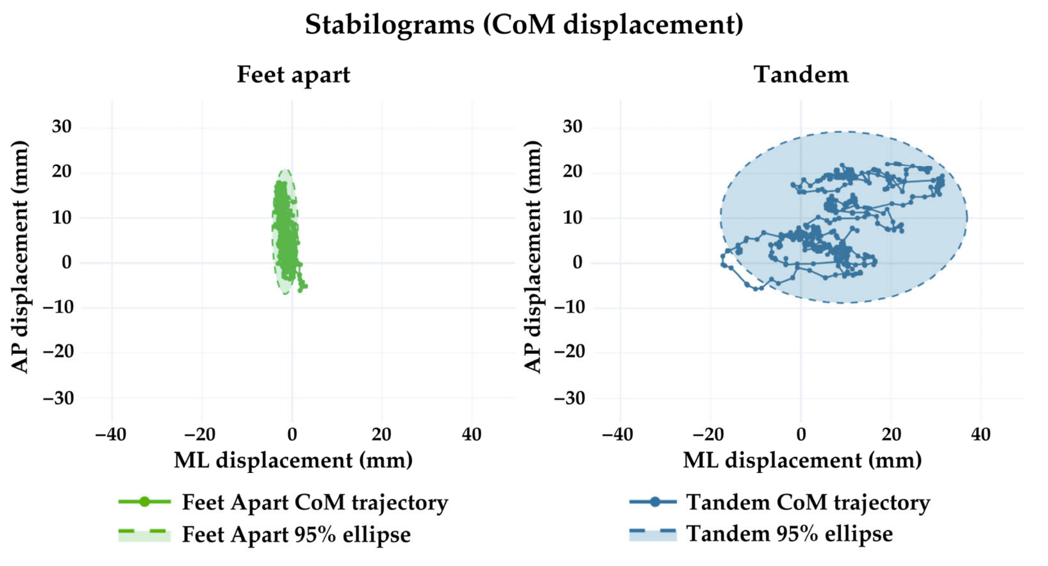

Figure 7. Example of stabilograms of Feet apart and Tandem balance stances.

Given the differences in base of support, each metric is annotated with its corresponding stance. Direct comparisons are more meaningful between subjects in the same stance than across different stances.

It is important to note that for each balance posture, the initial position (i.e., the zero reference point) is determined by averaging the CoM position of the first 3 s of the test.

This early phase estimation ensures that subsequent measurements of displacement and sway are relative to a stable and consistent starting position.

These objective measurements complement the simple observation of whether the subject can maintain the posture, providing a richer profile of their postural stability.

2.4. Inclusion and Exclusion Criteria

Participants were included if they were aged 65 years or older, could stand independently for at least 30 s with or without assistive devices, and could understand simple verbal instructions. Participants were excluded if they had acute musculoskeletal injuries, severe cognitive impairment, or any condition that contraindicated participation in light physical activities.

All participants gave written informed consent.

2.5. Clinical Assessment

Scores for the Tinetti Performance-Oriented Mobility Assessment (POMA) [21,22] and the modified Barthel Index (mBI) [23,24] were extracted from each participant's most recent comprehensive evaluation performed $\leq$ months before Kinect testing by the nursing-home physiotherapy and nursing team. The 16-item POMA (9-item balance, 7-item gait), rated on a 0–2 scale, yields a maximum of 28 points; scores ≤ 24 indicate elevated fall-risk. The 10-item mBI (five-level rating; range 0–100) evaluates independence in basic activities of daily living (ADL). Internal consistency and sensitivity are superior to the original Barthel Index in older cohorts.

2.6. Statistical Analysis

The statistical plan was structured around the two primary research objectives. Objective 1 (technical feasibility in older adults) was addressed by summarizing, for the older group, knee-flexion, CoM-sway and squat-depth metrics and by testing whether their distributions met the expected biomechanical ranges reported in the literature (see H_{0a}). Objective 2 (systematic comparison with young adults) was tackled through between-group tests (H_{0b}) and within-subject repeated-measure tests to quantify stability of the metrics over time. The specific non-parametric procedures selected for each hypothesis are detailed below.

All statistical analyses were performed in Python 3.12 (Pandas 2.2, SciPy 1.14, Pingouin 0.5). Data normality was examined with the Shapiro–Wilk test. Because at least one variable per domain violated normality ($p < 0.05$) and the sample size was below thirty, non-parametric methods were selected.

- Between-group comparison (Older vs. Young): The independent Older vs. Young comparison was performed with the Mann–Whitney U test. Results are reported as the U statistic, the two-tailed p-value, and Cohen's d, calculated with the pooled standard deviation of the two groups to quantify the magnitude of the difference.
- Repeated-measures comparison: To examine changes across the three consecutive 10-s windows (0–10 s, 10–20 s, 20–30 s) within each participant, a Friedman test was applied. When the omnibus test reached significance, Bonferroni-adjusted Wilcoxon signed-rank tests identified the specific pairs that differed. The global effect size for the Friedman test is given as Kendall's W (0 indicating no agreement, 1 indicating complete agreement).
- Significance threshold: All tests were two-tailed with $\alpha = 0.05$.
- Type II error risk: Given the exploratory nature of this pilot ($n = 8$ older, $n = 8$ young), statistical power is limited; p-values close to 0.05 should therefore be interpreted

cautiously. Effect-size estimates (Cohen's d and Kendall's W) are provided to aid interpretation until larger validation studies can be conducted.

Working hypotheses:

- H_{0a}: there is no difference between older and young adults in quantitative squat performance (minimum knee angle, CoM vertical displacement, Squat Index).
- H_{0b}: there is no difference between groups in postural-sway metrics (ML/AP displacements, 95% CoM-ellipse area) during static stances.

Rejection of either null hypothesis would support the technological feasibility of Azure Kinect to capture clinically relevant lower-limb and balance variables, thereby fulfilling Objectives 1–2.

2.7. Experimental Setup

The evaluations were conducted in a large room at the nursing home. The sensor (Azure Kinect) was mounted at a height of approximately 1 m and positioned 2–3 m away from the participant to ensure that the entire body was within the field of view. The room had neutral lighting and sufficient space.

Walking aids were removed from the base of support and placed behind the participant; all exercises were therefore executed unaided while a member of the study team provided standby supervision.

3. Results

3.1. Participant Characteristics

A preliminary evaluation was conducted with eight older adults (five women and three men) residing in a nursing home, with ages ranging from 71 to 94 years (median = 88.5 years; IQR = 80.8–92.0). Over a 7-week period, each participant was measured on nine occasions (two sessions per week during the first two weeks, followed by one session per week thereafter). These participants exhibited varying levels of physical fitness yet remained largely independent in their activities of daily living, as indicated by Modified Barthel Index scores close to 100 (median = 98; IQR = 95–100; range 90–100). Despite this functional independence, median Tinetti POMA was 26 (IQR = 24.5–28, range 23–28), indicating some gait-balance limitations; five of the eight volunteers used walking aids, and several reported at least one fall in the previous year. Detailed demographic and clinical data, including fall history, are presented in Table 2.

Table 2. Characteristics of older volunteers.

Age (Years)	Gender	Walking Aid	Tinetti	Barthel	Falls	
					Previous [1]	During [2]
87	Female	None	28	97	0	0
90	Female	Cane	23	98	0	0
92	Female	Cane	26	93	0	1
94	Female	Walker	26	90	5	1
71	Male	None	28	100	0	0
84	Male	Wheelchair	23	N/A	0	0
71	Male	None	28	100	4	0
92	Female	Walker	25	100	1	0

Summary statistics for the eight older participants: Age—median 88.5 (IQR 80.8–92; range 71–94); Tinetti—median 26 (IQR 24.5–28; range 23–28); Barthel—median 98 (IQR 95–100; 90–100). [1] Falls that occurred during the year prior to the start of the study. [2] Falls that occurred during the measurement sessions of the study.

It is worth noting that the participants' high Barthel and Tinetti scores indicate a relatively well-preserved functional status despite advanced age, although the presence of walking aids and previous falls suggests some degree of mobility impairment typical of older populations.

To provide a comparative benchmark, a sample of eight younger adults (three women and five men) aged 26 to 55 years was also recruited. None presented known musculoskeletal or balance disorders. Their baseline data can be found in Table 3. This younger cohort served as a control group, helping to determine whether the proposed platform could distinguish expected age-related differences in lower-limb strength (squatting tasks) and postural stability (static balance tests).

Table 3. Characteristics of younger volunteers.

Age (Years)	Gender
33	Male
34	Female
26	Female
26	Male
26	Female
26	Male
38	Male
55	Male

Informed consent was obtained prior to testing and it was verified that they could perform a partial squat and hold the semitandem position safely.

3.2. Comparison Between Older and Younger Adults

All participants completed the two main test protocols (self-selected depth squats and four progressively challenging static balance stances) while being tracked by the Azure Kinect sensor. A series of biomechanical metrics were extracted (Section 2.3), including the vertical displacement of the CoM during squats, knee angles, a spinal alignment index, symmetry indices for bilateral leg motion, and postural sway indicators during static balance.

To explore the platform's ability to differentiate between age groups, the metrics were compared following the analysis plan outlined in Section 2.6. Noteworthy findings are summarized below:

1. Squat Depth, Knee Flexion Angles and Squat Index:

The platform captured a clear tendency for older adults to exhibit less vertical displacement of the CoM during squats ($p < 0.001$), indicating more limited descent compared to the younger group. Correspondingly, their minimum knee angles (left and right) were significantly larger ($p < 0.001$), reflecting reduced knee flexion. For instance, the median minimum knee angle in the older group was about 110°, whereas the younger group reached about 60°. The calculated squat index, which combines both depth and repetition count, was also significantly lower in the older adults ($p < 0.001$). This underscores the reduced overall squatting performance potentially linked to age-related declines in lower-extremity strength and range of motion.

2. Spinal Alignment and Symmetry: No statistically significant differences were observed in the spinal alignment index ($p = 0.645$) or the symmetry index ($p = 0.505$) between the groups. This suggests that, although older adults descend less, their squat technique or distribution of load (left vs. right) may remain relatively balanced, and they do not exhibit marked asymmetries in knee flexion when performing the movement.
3. Static Balance Metrics: Static-balance metrics showed significant differences in several postural sway metrics between the older and younger adults. Specifically, older

adults showed greater maximum ML displacement (p = 0.01), greater mean ML displacement (p = 0.015), greater maximum AP displacement (p < 0.001) and greater mean AP displacement (p < 0.001). The CoM trajectory ellipse area (a 95% confidence ellipse) was also significantly larger in older adults (p < 0.001).

Overall, these findings indicate that the proposed platform effectively differentiates older from younger adults in terms of squat depth and postural stability. Table 4 provides a detailed breakdown of the relevant U statistics and p-values, while Figure 8 illustrates some of these group-wise differences in squat and balance metrics.

Table 4. Comparison results of Biomechanical Metrics Between Older and Younger Adults using the Mann–Whitney U Test.

	Metric	Older Median	Younger Median	U Statistic	p-Value [1]	Cohen's d
Squats	Mean disp. in X-axis (mm)	2.44	−3.04	43	0.279	−0.02
	Mean disp. in Z-axis (mm)	−9.05	3.09	20	0.234	−0.42
	Mean disp. in Y-axis (mm)	−51.83	−142.27	64	<0.001	3.56
	Min. Knee Angle Left (°)	109.19	57. 93	64	<0.001	3.38
	Min. Knee Angle Right (°)	110.82	60. 97	64	<0.001	3.73
	Spinal Alignment	170.29	169.45	37	0.645	0.28
	Symmetry Index	3.38	2.68	39	0.505	0.20
	Number of squats	16.50	14.50	42	0.317	0.26
	Max. disp. in Y-axis (mm)	143.63	366.17	0	<0.001	−3.73
	Squat Index	1756.31	5401.51	1	<0.001	−3.12
Balance (10 s)	Max. ML Disp. (mm)	7.82	6.74	56	0.010	1.40
	Mean ML Disp. (mm)	3.37	2.48	55	0.015	1.40
	Max. AP Disp. (mm)	9.14	7.03	62	<0.001	2.16
	Mean AP Disp. (mm)	3.51	2.76	62	<0.001	2.23
	CoM Trajectory Ellipse Area (mm^2)	191.13	128.31	60	0.002	1.19

[1] p-values < 0.001 are reported as such for clarity.

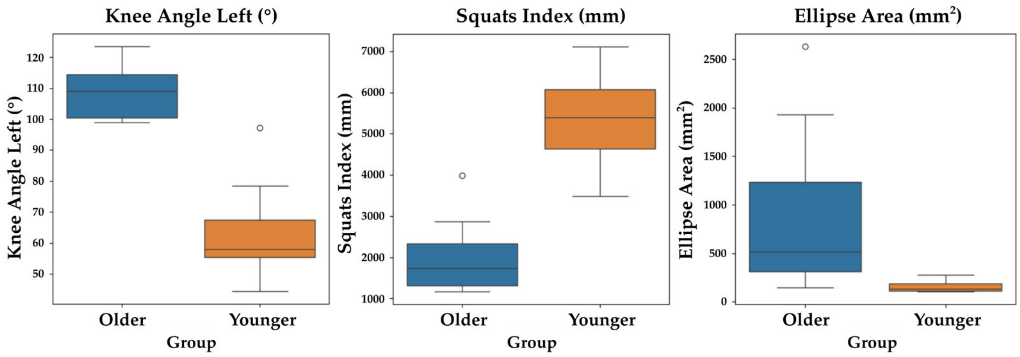

Figure 8. Comparison Results—box plots of knee angle range (degrees), squat index (dimensionless) and sway ellipse area (mm^2) in older (n = 8) and young (n = 8) participants.

3.3. 10-s vs. 30-s Balance Analysis

All participants were measured for 30 s in each balance posture (Feet Apart, Feet Together, Semitandem, and Tandem). During this period, the CoM) was continuously tracked. Figure 9 presents the group-averaged CoM displacement in ML and AP directions (±1 standard deviation) over the 30 s interval for each stance, combining all valid recordings.

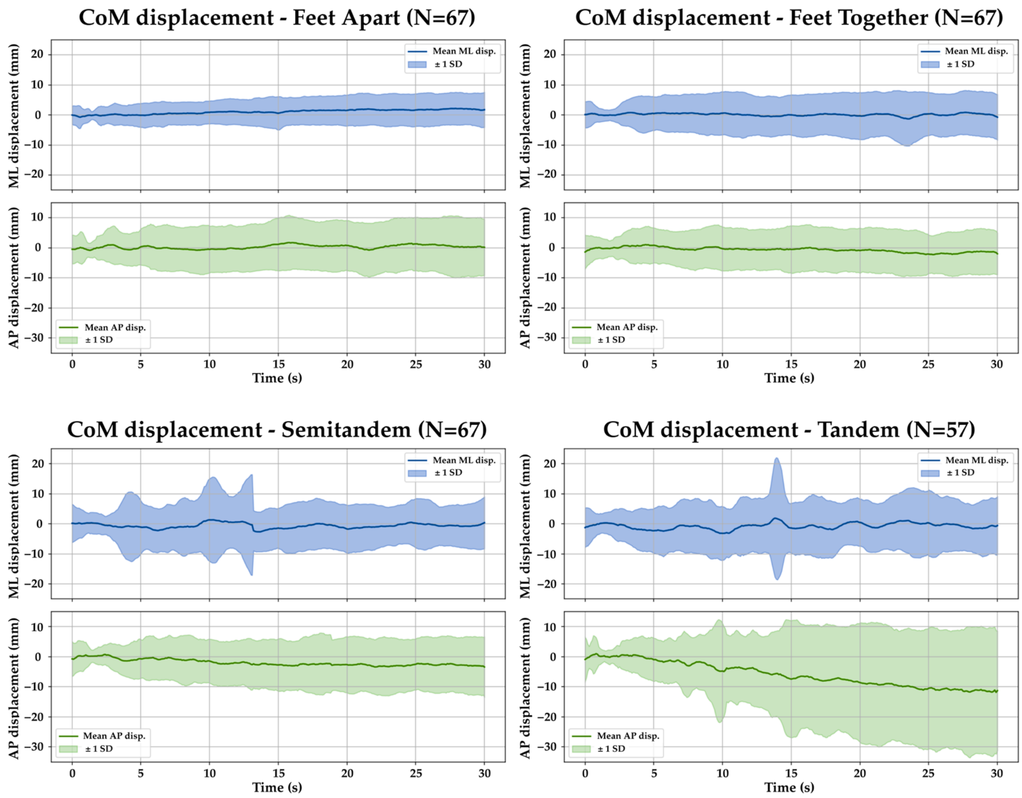

Figure 9. Group-Averaged CoM displacement in ML and AP directions during 30 s balance trials.Visual inspection suggests that the most pronounced fluctuations occur in the initial phase of each instance, with Tandem typically exhibiting wider variability due to its higher level of difficulty.

To formally assess whether the earliest portion of the trial (0–10 s) suffices to characterize each participant's sway, the 30 s were partitioned into three consecutive 10 s windows (0–10 s, 10–20 s, and 20–30 s) and a 95% confidence ellipse area was calculated in each window. Table 5 summarizes the results of a Friedman test for repeated measures. In every stance, Friedman revealed significant differences ($p < 0.05$) among the three intervals, indicating that at least one window diverges from the others.

Table 5. Friedman test and Wilcoxon pairwise (see Section 2.6) comparisons results for ellipse area across three consecutive 10-s windows.

Stance	χ^2 (*p*-Value)	Kendall's W	Window Pair	W-Stat	*p*-Corrected
Feet apart	6.75 (0.034)	0.578	0–10 vs. 10–20	1	0.047
			0–10 vs. 20–30	1	0.047
			10–20 vs. 20–30	12	1.000
Feet together	9.25 (0.010)	0.422	0–10 vs. 10–20	0	0.023
			0–10 vs. 20–30	5	0.234
			10–20 vs. 20–30	14	1.000
Semitandem	10.75 (0.005)	0.672	0–10 vs. 10–20	4	0.164
			0–10 vs. 20–30	0	0.023
			10–20 vs. 20–30	3	0.117
Tandem	8.857 (0.011)	0.633	0–10 vs. 10–20	7	0.891
			0–10 vs. 20–30	0	0.047
			10–20 vs. 20–30	9	1.000

Across all four static stances, the Friedman test revealed significant differences in the 95% CoM ellipse area among the three consecutive 10 s windows (feet apart $\chi^2(2) = 6.75$, $p = 0.034$; feet together $\chi^2(2) = 9.25$, $p = 0.010$; semitandem $\chi^2(2) = 10.75$, $p = 0.005$; tandem $\chi^2(2) = 8.86$, $p = 0.011$; Kendall's W ranging from 0.422 to 0.672; Table 5). Bonferroni-adjusted Wilcoxon pairwise tests (Table 5) showed that the 0–10 s window differed significantly from at least one later window in every stance (p-corrected ≤ 0.047), whereas the 10–20 s and 20–30 s windows seldom differed (p-corrected ≥ 0.117 in all 4 relevant comparisons; Table 5).

3.4. Longitudinal Case Examples

To illustrate the utility of our platform in detecting changes in postural control over time—and to provide a richer clinical context—two case examples are presented in Figure 10. For each participant (ID 1 and ID 4), the session-by-session number of squats, mean squat depth and mean CoM displacement metrics for Tandem stance are shown, alongside relevant clinical characteristics.

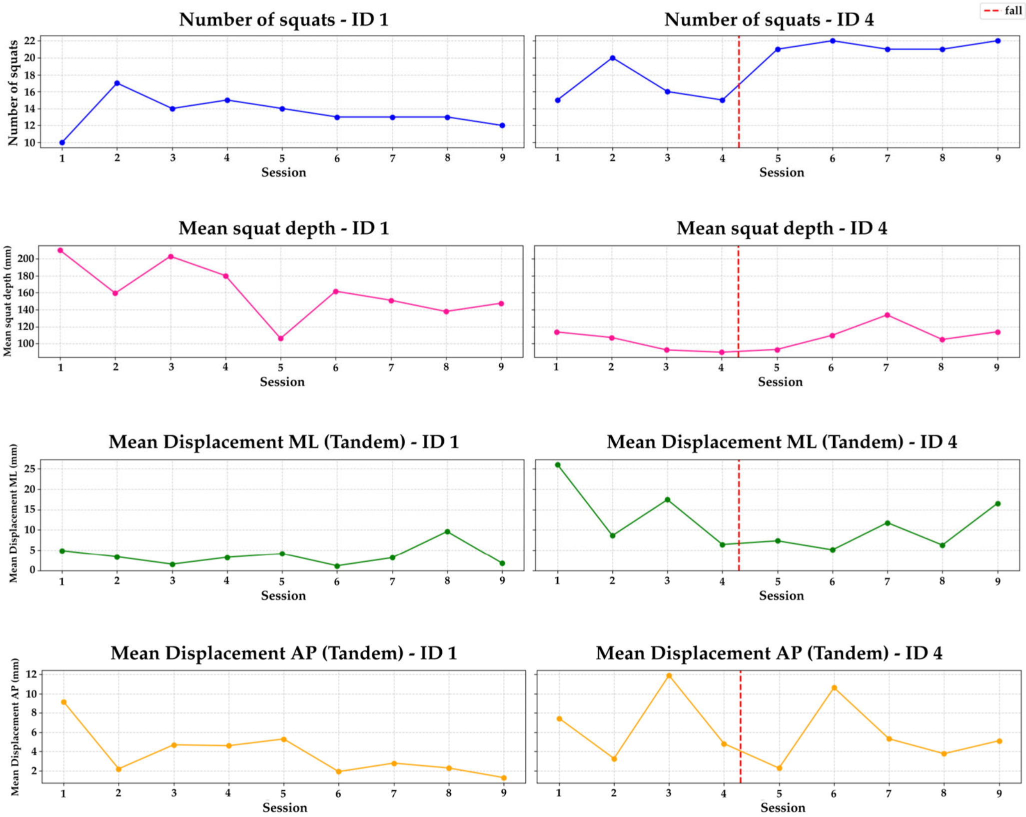

Figure 10. Longitudinal case examples: session-by-session changes in squat performance and tandem balance metrics. Colour coding: blue = number of squats; pink = mean squat depth; green = mean mediolateral (ML) displacement; orange = mean anteroposterior (AP) displacement. The vertical dashed red line marks the session in which a fall occurred.

Participant ID 1 (Age: 87; No walking aid; Tinetti score = 28; Barthel Index = 97; No falls) exhibited relatively stable performance across nine sessions. The mean CoM displacement in both the ML and AP directions remained consistent over time, with only modest fluctuations in squat performance and tandem-stance sway. This stability aligns with the favorable clinical profile of ID 1, who, despite advanced age, demonstrates high functional scores and absence of falls.

In contrast, Participant ID 4 (Age: 94; Walking aid: Walker; Tinetti score = 26; Barthel Index = 90; 5 falls in the year prior to the study and 1 fall during the study) displayed marked variability. Notably, a fall occurred between Sessions 4 and 5 (indicated by a vertical dashed line in Figure 10). Following this event, the tandem-stance sway metrics (both ML and AP) fluctuated more noticeably, and squat performance also varied from session to session. These findings suggest that the fall—and the participant's more compromised clinical status—may have contributed to the increased instability and variability observed over time.

By integrating these clinical characteristics, our analysis underscores the value of a longitudinal monitoring system that not only captures immediate postural adaptations (especially within the first 10 s) but also contextualizes them within the overall functional status of the individual. Such detailed insight can help clinicians tailor interventions more precisely, for instance, by identifying individuals (like ID 4) who may benefit from targeted balance training or fall-prevention strategies.

4. Discussion

In this study, we developed and tested a non-contact functional evaluation platform based on the Azure Kinect to assess lower-limb functional performance and balance in older adults through simple and clinically relevant tasks. Our approach leverages markerless motion capture to extract quantitative metrics—such as squat depth, knee angles and postural sway—which are essential for evaluating mobility and fall risk. Similar to recent advances in sensor-based frailty monitoring [25–27], our system aims to complement traditional clinical assessments by providing objective, high-resolution data during routine physical tasks. These findings fulfill Objective 1 by confirming technical feasibility, address Objective 2 through systematic older-versus-young comparisons (Section 3.2), and meet Objective 3 by revealing early phase sway (Section 3.3) and longitudinal variability (Figure 10) as indicators of incipient decline.

This study's goal regarding falls (Objective 3) was intentionally exploratory: our aim was only to verify that the Azure Kinect can in principle capture metrics linked to balance and lower-limb performance, not to derive fall predictors in a heterogeneous older sample. The presence of walking aids and previous falls in our cohort confirms a spectrum of impairment that the system can quantify, yet—given the small N—we purposely refrain from interpreting individual differences. A definitive evaluation of fall-risk metrics will require larger samples and subgroup analyses (e.g., older adults with vs. without a fall history or different frailty levels), which we have already planned for future work.

Our results indicate that the system reliably distinguishes between varying levels of functional performance. The squat test, quantified by the vertical displacement of the CoM, the number of squats and the minimum knee angles, consistently demonstrated that older adults perform shallower squats compared to younger individuals. This finding is consistent with previous reports that document reduced lower-extremity strength and joint mobility with advancing age [28]. By allowing participants to squat to a self-selected depth, we minimized discomfort yet still observed clear performance gaps relative to younger adults. We did not detect large asymmetries in knee flexion—suggesting that many older adults in this cohort maintained balanced bilateral usage, despite performing fewer and less complete squat cycles overall. These metrics complement traditional functional measures (e.g., the TUG, the 30 s chair stand or the SPPB) by providing additional parameters like knee angles or continuous motion trajectories, thereby enabling clinicians to detect subtler changes in mobility.

In the static balance tasks, the older group exhibited greater ML and AP sway, as evidenced by increased displacement metrics and larger 95% confidence ellipse areas. The greater sway observed in older adults is consistent with well-documented age-related declines in postural control [21–23]. These observations confirm that age-related sensorimotor degradation leads to diminished postural stability—a finding in line with prior investigations in geriatric populations [29–31]. While many standardized tests (e.g., Short Physical Performance Battery) rely on whether an individual can simply maintain a stance, our platform goes a step further by quantifying not just pass/fail but also the extent of sway in each stance. This additional resolution may be particularly valuable in identifying emerging balance problems at earlier stages.

Window-specific analysis showed that the 95% CoM ellipse-area was largest during the first 10 s of each stance and then plateaued; pairwise comparisons confirmed that 10–20 s seldom differed from 20–30 s, whereas 0–10 s differed from at least one later window in every stance. This pattern helps explain why brief 10-s balance tasks—such as the standing component of the Short Physical Performance Battery (SPPB) [9]—are able to expose postural instability so efficiently: they capture the most demanding adaptation phase, when individuals are still seeking equilibrium. Conversely, if the clinical aim is to characterize steady-state balance once the posture has stabilized, analyzing sway after the initial 10 s (for example, in the 10–20 s interval) appears sufficient; extending recordings to a full 30 s adds little additional information while lengthening test time.

Furthermore, our longitudinal observations highlight that repeated assessments can help track gradual or event-related changes in performance. One participant (ID 4) who had a walker and multiple fall incidents showed relatively large fluctuations in tandem-stance sway across sessions—particularly following an intervening fall. This variability contrasts with a more stable participant (ID 1), whose balance metrics remained consistent. Although our sample was small, this case-to-case difference underscores how a simple, markerless system could be used to monitor older adults over weeks or months, detecting fluctuations that traditional one-time evaluations might overlook. Previous research on wearable sensor-based monitoring has shown the value of repeated measures for anticipating and potentially preventing mobility-related incidents [25,26], and the present work suggests a similar strategy could be feasible with markerless devices. Each participant was tested at most once per day with rest between tasks, and no systematic practice or fatigue effect was evident (e.g., ID 1 remained stable across nine sessions). Larger longitudinal datasets will enable mixed-effects modelling that explicitly accounts for learning and fatigue.

However, several limitations must be acknowledged. First, our sample size was small (N = 8 per group), and the older cohort, while very aged, was relatively high-functioning (most had good baseline scores and few were recurrent fallers). Second, although prior studies have reported acceptable agreement between Kinect-based and laboratory-grade systems for measuring gait, joint angles, and balance [11,12,32], we did not perform a direct comparison with gold-standard motion capture or force plates. Future research with larger and more varied geriatric populations, including frailer individuals and those with a history of recurrent falls, as well as formal accuracy benchmarking, would help validate and extend these preliminary results.

Although the older adults in our sample exhibited the expected deficits relative to the young cohort—supporting the system's construct validity—this pilot study was not intended to establish new clinical indices or to delineate unique functional characteristics of older adults. Such finer-grained analyses will be pursued once a larger, clinically stratified dataset becomes available.

This platform, which requires minimal setup, operates with a non-contact design, and involves brief testing protocols, could be readily adopted in resource-limited settings such as community clinics or nursing homes, and it could enable early detection of mobility decline and promote targeted fall prevention strategies or strengthening interventions.

5. Conclusions

This pilot study demonstrates the feasibility of a simple, markerless Azure Kinect platform to capture quantitative squat and sway metrics in older adults without wearable sensors or specialized laboratories, and it reliably discriminated between eight older and eight younger participants by revealing shallower squat depth, larger minimum knee angles, and greater CoM sway in the older group. These results satisfy Objective 1, confirming that the system can acquire valid biomechanical data in older adults, and Objective 2, showing it can systematically differentiate them from young healthy controls. Crucially, the window-specific balance analysis—where the first ten seconds of each stance already exposed peak instability—and the session-to-session variability observed after a real fall illustrate the platform's capacity to flag subtle functional changes at an early stage, thereby fulfilling Objective 3 of exploring its potential for early detection of physical decline. Although validation in larger, clinically stratified cohorts and benchmarking against gold-standard instruments are still needed, the present findings point to a practical, non-contact solution that could enrich routine geriatric assessment with fine-grained biomechanical information and ultimately support targeted fall-prevention strategies.

Author Contributions: Conceptualization, A.S.-S., P.A., C.F.-V., R.G.-G., J.M.L.-H., L.R.-C. and A.C.; methodology, A.S.-S., C.F.-V. and L.R.-C.; software, A.S.-S. and P.A.; validation, A.S.-S. and P.A.; formal analysis, A.S.-S., P.A. and A.C.; investigation, A.S.-S. and C.F.-V.; resources, J.M.L.-H., L.R.-C. and A.C.; data curation, A.S.-S.; writing—original draft preparation, A.S.-S.; writing—review and editing, C.F.-V., R.G.-G., J.M.L.-H., L.R.-C. and A.C.; visualization, A.S.-S., P.A. and C.F.-V.; supervision, J.M.L.-H. and L.R.-C.; project administration, J.M.L.-H., L.R.-C. and A.C.; funding acquisition, R.G.-G., J.M.L.-H., L.R.-C. and A.C. All authors have read and agreed to the published version of the manuscript.

Funding: This work was supported by projects CPP2022-009714 funded by MICIU/AEI/10.13039/501100011033 and EU NextGenerationEU/PRTR; and PID2022-137269OB-C22 funded by MICIU/AEI/10.13039/501100011033 and FEDER, EU.

Institutional Review Board Statement: The study was conducted in accordance with the Declaration of Helsinki, and approved by the Committee on Ethics in Research with Medical Products of Cantabria (CEIm) (protocol code CPP2022-009714; approval date: 19 July 2024).

Informed Consent Statement: Informed consent was obtained from all subjects involved in the study.

Data Availability Statement: The datasets generated and/or analyzed during the current study are available from the corresponding author upon reasonable request.

Acknowledgments: The authors gratefully acknowledge the Nursing and Physiotherapy team at the San Cándido Foundation (Santander) for their collaboration and assistance during the data collection process. We also thank A. Perez Asensio and B. García García for their support during the measurements.

Conflicts of Interest: Author Roberto García-García is employed by the company Ambar Telecomunicaciones S.L. The remaining authors declare that the research was conducted in the absence of any commercial or financial relationships that could be construed as a potential conflict of interest.

Abbreviations

The following abbreviations are used in this manuscript:

AP	Anteroposterior
CoM	Center of Mass
CSV	Comma-Separated Values
GPU	Graphics Processing Unit
ML	Mediolateral

ToF	Time of Flight
TUG	Timed Up-and-Go
RGB	Red, Green, Blue
SDK	Software Development Kit
SI	Symmetry Index
SPPB	Short Physical Performance Battery

References

1. Ageing and Health. Available online: https://www.who.int/news-room/fact-sheets/detail/ageing-and-health (accessed on 3 March 2025).
2. Salari, N.; Darvishi, N.; Ahmadipanah, M.; Shohaimi, S.; Mohammadi, M. Global Prevalence of Falls in the Older Adults: A Comprehensive Systematic Review and Meta-Analysis. *J. Orthop. Surg. Res.* **2022**, *17*, 334. [CrossRef]
3. Nagano, H. Gait Biomechanics for Fall Prevention among Older Adults. *Appl. Sci.* **2022**, *12*, 6660. [CrossRef]
4. Marques, N.R.; Spinoso, D.H.; Cardoso, B.C.; Moreno, V.C.; Kuroda, M.H.; Navega, M.T. Is It Possible to Predict Falls in Older Adults Using Gait Kinematics? *Clin. Biomech.* **2018**, *59*, 15–18. [CrossRef] [PubMed]
5. Vaishya, R.; Vaish, A. Falls in Older Adults Are Serious. *JOIO* **2020**, *54*, 69–74. [CrossRef] [PubMed]
6. Patrizio, E.; Calvani, R.; Marzetti, E.; Cesari, M. Physical Functional Assessment in Older Adults. *J. Frailty Aging* **2021**, *10*, 141–149. [CrossRef] [PubMed]
7. Herman, T.; Giladi, N.; Hausdorff, J.M. Properties of the 'Timed Up and Go' Test: More than Meets the Eye. *Gerontology* **2010**, *57*, 203–210. [CrossRef]
8. Jones, C.J.; Rikli, R.E.; Beam, W.C. A 30-s Chair-Stand Test as a Measure of Lower Body Strength in Community-Residing Older Adults. *Res. Q. Exerc. Sport.* **1999**, *70*, 113–119. [CrossRef]
9. Guralnik, J.M.; Simonsick, E.M.; Ferrucci, L.; Glynn, R.J.; Berkman, L.F.; Blazer, D.G.; Scherr, P.A.; Wallace, R.B. A Short Physical Performance Battery Assessing Lower Extremity Function: Association With Self-Reported Disability and Prediction of Mortality and Nursing Home Admission. *J. Gerontol.* **1994**, *49*, M85–M94. [CrossRef]
10. Ortega-Bastidas, P.; Gómez, B.; Aqueveque, P.; Luarte-Martínez, S.; Cano-de-la-Cuerda, R. Instrumented Timed Up and Go Test (iTUG)—More Than Assessing Time to Predict Falls: A Systematic Review. *Sensors* **2023**, *23*, 3426. [CrossRef]
11. Clark, R.A.; Pua, Y.-H.; Fortin, K.; Ritchie, C.; Webster, K.E.; Denehy, L.; Bryant, A.L. Validity of the Microsoft Kinect for Assessment of Postural Control. *Gait Posture* **2012**, *36*, 372–377. [CrossRef]
12. Eltoukhy, M.A.; Kuenze, C.; Oh, J.; Signorile, J.F. Validation of Static and Dynamic Balance Assessment Using Microsoft Kinect for Young and Elderly Populations. *IEEE J. Biomed. Health Inform.* **2018**, *22*, 147–153. [CrossRef] [PubMed]
13. Jeyasingh-Jacob, J.; Crook-Rumsey, M.; Shah, H.; Joseph, T.; Abulikemu, S.; Daniels, S.; Sharp, D.J.; Haar, S. Markerless Motion Capture to Quantify Functional Performance in Neurodegeneration: Systematic Review. *JMIR Aging* **2024**, *7*, e52582. [CrossRef]
14. Azure Kinect DK: Desarrollo de Modelos de IA | Microsoft Azure. Available online: https://azure.microsoft.com/es-es/products/kinect-dk (accessed on 2 April 2025).
15. Winter, D.A. *Biomechanics and Motor Control of Human Movement*, 4th ed.; John Wiley & Sons, Inc.: Hoboken, NJ, USA, 2009.
16. de Leva, P. Adjustments to Zatsiorsky-Seluyanov's Segment Inertia Parameters. *J. Biomech.* **1996**, *29*, 1223–1230. [CrossRef]
17. Zatsiorsky, V.M.; Seluyanov, V.N.; Chungunova, L.G. Methods of Determining Mass-Inertial Characteristics of Human Body Segments. In *Contemporary Problems of Biomechanics*; CRC Press: Boca Raton, FL, USA, 1990; pp. 272–291.
18. Gill, N.; Preece, S.J.; Young, S.; Bramah, C. Are the Arms and Head Required to Accurately Estimate Centre of Mass Motion during Running? *Gait Posture* **2017**, *51*, 281–283. [CrossRef] [PubMed]
19. Błażkiewicz, M.; Wiszomirska, I.; Wit, A. Comparison of Four Methods of Calculating the Symmetry of Spatial-Temporal Parameters of Gait. *Acta Bioeng. Biomech.* **2014**, *16*, 29–35. [CrossRef]
20. Find_peaks—SciPy v1.15.2 Manual. Available online: https://docs.scipy.org/doc/scipy/reference/generated/scipy.signal.find_peaks.html (accessed on 1 April 2025).
21. Tinetti, M.E. Performance-Oriented Assessment of Mobility Problems in Elderly Patients. *J. Am. Geriatr. Soc.* **1986**, *34*, 119–126. [CrossRef]
22. Scura, D.; Munakomi, S. Tinetti Gait and Balance Test. In *StatPearls*; StatPearls Publishing: Treasure Island, FL, USA, 2025.
23. Mahoney, F.I.; Barthel, D.W. Functional Evaluation: The Barthel Index. *Md. State Med. J.* **1965**, *14*, 61–65. [PubMed]
24. Shah, S.; Vanclay, F.; Cooper, B. Improving the Sensitivity of the Barthel Index for Stroke Rehabilitation. *J. Clin. Epidemiol.* **1989**, *42*, 703–709. [CrossRef]
25. Park, C.; Sharafkhaneh, A.; Bryant, M.S.; Nguyen, C.; Torres, I.; Najafi, B. Toward Remote Assessment of Physical Frailty Using Sensor-Based Sit-to-Stand Test. *J. Surg. Res.* **2021**, *263*, 130–139. [CrossRef]

26. Arshad, M.Z.; Jamsrandorj, A.; Kim, J.; Mun, K.-R. Gait Events Prediction Using Hybrid CNN-RNN-Based Deep Learning Models through a Single Waist-Worn Wearable Sensor. *Sensors* **2022**, *22*, 8226. [CrossRef]
27. Friedrich, B.; Lau, S.; Elgert, L.; Bauer, J.M.; Hein, A. A Deep Learning Approach for TUG and SPPB Score Prediction of (Pre-) Frail Older Adults on Real-Life IMU Data. *Healthcare* **2021**, *9*, 149. [CrossRef]
28. Honda, K.; Sekiguchi, Y.; Shimazaki, S.; Suzuki, R.; Suzuki, T.; Kanetaka, H.; Izumi, S.-I. Effects of Aging on Whole-Body Center of Mass Movement and Lower Limb Joint Kinematics and Kinetics during Deep-Squat Movement. *J. Biomech.* **2022**, *134*, 110996. [CrossRef] [PubMed]
29. Prieto, T.E.; Myklebust, J.B.; Hoffmann, R.G.; Lovett, E.G.; Myklebust, B.M. Measures of Postural Steadiness: Differences between Healthy Young and Elderly Adults. *IEEE Trans. Biomed. Eng.* **1996**, *43*, 956–966. [CrossRef] [PubMed]
30. Seidler, R.D.; Bernard, J.A.; Burutolu, T.B.; Fling, B.W.; Gordon, M.T.; Gwin, J.T.; Kwak, Y.; Lipps, D.B. Motor Control and Aging: Links to Age-Related Brain Structural, Functional, and Biochemical Effects. *Neurosci. Biobehav. Rev.* **2010**, *34*, 721–733. [CrossRef] [PubMed]
31. Sturnieks, D.L.; St George, R.; Lord, S.R. Balance Disorders in the Elderly. *Neurophysiol. Clin. Clin. Neurophysiol.* **2008**, *38*, 467–478. [CrossRef]
32. Albert, J.A.; Owolabi, V.; Gebel, A.; Brahms, C.M.; Granacher, U.; Arnrich, B. Evaluation of the Pose Tracking Performance of the Azure Kinect and Kinect v2 for Gait Analysis in Comparison with a Gold Standard: A Pilot Study. *Sensors* **2020**, *20*, 5104. [CrossRef]